GLOBAL SURVEY OF WELL-PRESERVED MARTIAN CRATERS IN THE SIMPLE-TO-COMPLEX TRANSITION. R. R. Herrick[1], L. M. Dorn[1], and B. M. Hynek[2], [1]Geophysical Institute, University of Alaska Fairbanks, Fairbanks AK 99775-7320 (rrherrick@alaska.edu), [2]Laboratory for Atmospheric and Space Physics and Geological Sciences, University of Colorado, 3665 Discover Drive, Boulder, CO 80303 (hynek@lasp.colorado.edu).

Introduction: We have been examining similar-sized impact craters in the diameter range of the global simple-to-complex transition for the Moon and Mars [1,2,3]. For a given planet, examining a family of impact craters of similar diameter is empirically the closest one can come to holding impact energy constant to test for the effects of varying target and impact conditions on final crater morphology. The morphology variation can be maximized by examining differences between craters at the diameter of a key transition such as that between simple and complex craters. In previous work, Herrick and Hynek [1] relied on the database of Robbins and Hynek [4] to draw statistical associations between crater types and different geologic units for craters in this transition, $7 < D < 9$ km.

Because that database was compiled at a time when the only global image and topography data sets were THEMIS daytime IR (100 m/pixel) and gridded MOLA data (varying, ~1-2 km spatial resolution), the morphology descriptions and depth measurements were problematic. Now that global CTX coverage (6 m/pixel) and a blended HRSC/MOLA data set are available, we have reexamined and reclassified the morphology of the best-preserved craters and reassessed their rim-floor depths. In a companion abstract [Dorn and Herrick, this conference], we examine the details of some type examples using topography derived from CTX stereo pairs.

Methodology: In JMARS, for the 574 craters classified as Preservation State 4 (most pristine) in [4] with $7 < D < 9$ km we examined their morphologies using the global CTX mosaic of [5], supplemented with CTX and THEMIS Vis frames where additional imaging was required. Using the blended HRSC/MOLA gridded topography supplemented with the JMARS capability to plot MOLA measurements, we interpreted a representative rim/floor depth d for each crater. Main morphology classifications are as follows:

Floor morphology: Bowl-shaped (simple crater); central raised mound or peak; flat floor; central pit; ice-filled. The last category describes an otherwise fresh crater whose floor has been covered by ice-rich material [6] deposited well after crater formation through climatological processes.

Wall morphology: Smooth walls, minimally altered after excavation; material from the crater wall Slumps and is deposited on the floor; the wall fails in places along discrete faults and forms incipient or full Terraces; wall failure occurs along multiple discrete faults and extends to near crater center, which we call "Super-terraced" (example in Figure 1).

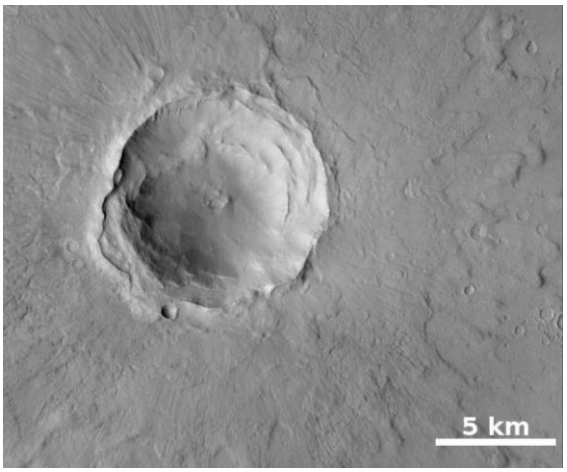

Figure 1 Martian impact crater at 41.47º N, 4.893º E, has a small central peak and continuous terracing to nearly crater center, a classification we call "super-terraced."

Ejecta: single-layer flow ejecta; double-layer; multiple layer; radial (ballistically emplaced). Many craters appear to have radial ejecta superposed by flow ejecta.

Tectonic control of crater shape: circular; minor tectonic control; tectonically controlled. "Minor" indicates that only a portion of the rim, < total 90° of arc, looks to have been controlled by faults or other discontinuities in the target near-surface and is straight or otherwise not a continuous arc.

Results: 45 of the craters were reclassified as being in a lower Preservation State and were discarded. The

Table 1. Matrix of floor morphologies (rows) and wall morphologies (columns) observed. Each cell shows (mean d/D, number of craters). Headings also show key to Figure 2 colors and shapes in parentheses.

Floor\wall	Smooth (circle)	Slumping (diamond)	Terraced (square)	Super-terraced (white square)
Bowl (yellow)	0.16, 24	0.19, 1	x	x
Central mound (blue)	0.11, 15	0.11, 51	0.09, 40	0.09, 7
Flat floor (orange)	0.11, 16	0.11, 151	0.10, 86	0.08, 3
Central pit (purple)	x	0.11, 32	0.10, 32	0.10, 1
Ice-filled (green)	0.09, 16	0.07, 8	0.08, 6	x

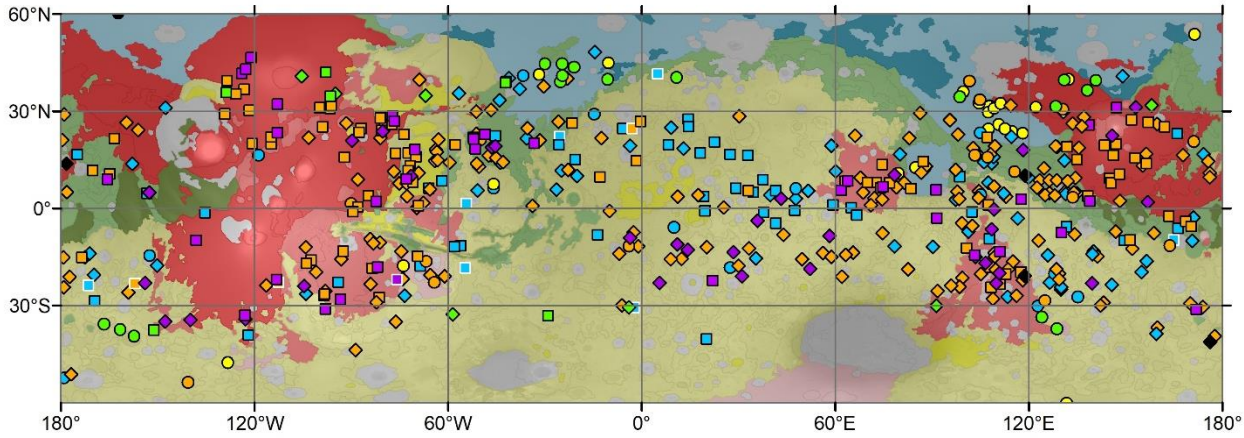

Figure 2. Well-preserved Martian craters with $7 < D < 9$ km in [4]. Color indicates floor morphology and shape indicates wall morphology; see Table 1 for key. Map is global geology from [7], simplified and superposed on gray-scale topography. Red areas are volcanic units (Dark red = Amazonian, medium red = Hesperian, light red = Noachian). Blue areas are lowlands units (dark blue = Amazonian, light blue = Hesperian). Green areas are transition units (dark green = Amazonian, light green = Hesperian). Yellow areas are highlands units (dark yellow = Hesperian, light yellow = Noachian). All other units are displayed in grey.

paucity of well-preserved craters near the poles (none above 60° latitude) and a few other regions coincides with areas of rapid degradation due to high near-surface ice content or high dust deposition. Table 1 shows a matrix of the mean rim-floor depths and sample number for different floor and wall morphologies, and Figure 2 shows the geographic distribution of these morphologies on a simplified global geologic map [7]. A rim-floor depth was not included in Table 1 if the crater formed on highly irregular topography (35 craters; e.g., the rim of a larger crater) or the crater floor was not sampled in topography (8 craters).

Figure 2 shows obvious associations between surface geology and crater morphology, with clustering in different geologic units beyond the simple color coding shown. A summary of key observations:

- Craters with a central mound/peak occur almost exclusively in nonvolcanic terrains.
- Simple craters, with high depths, occur almost exclusively in a few areas of the northern lowlands.
- There is clustering of wall behavior, but both slumping and coherent terraces occur with central mounds, central pits, and flat-floored craters, so different local conditions may control the nature of the central structure and the nature of wall failure.
- There are a few areas that bear examination as having exclusively central-pit craters, but the more typical occurrence is that central pit craters are mixed with flat-floored craters. Further examination is required to evaluate if the flat-floored craters in these mixed areas are just craters where the pits were filled by modest deposition, or if subtle local variations in geology cause a crater to end up with a central pit.
- Narrow ~10-degree bands (~30-40° latitude) define where the craters with ice-rich deposits occur.
- Lowlands and volcanic regions had higher percentage of circular craters, while craters with irregular, tectonically controlled rims are primarily found in highlands units.
- Our initial analysis has not shown a clear relationship between the morphology of flow-emplaced ejecta (single-, double-, multi-layered) and interior wall/floor morphology. However, the cases where flow ejecta appears to be emplaced over radial ejecta rarely occur in highlands units.

[Note: last two bullets are not shown in Figure 2]

Discussion and future work: The results here suggest clear ties between crater morphology and target cohesion, heterogeneity, and layering. The role of regional variations in near-surface volatile content is not so obvious. There are several craters in [4] that were classified as Preservation State 3 that are actually well-preserved that need to be added, and additional morphology/morphometry data needs to be collected. We are still synthesizing the work in order to pull out and interpret which aspects of the local geology control final crater appearance, and more importantly how that control is exerted.

References: [1] Herrick R. R. and Hynek B. M. (2017) *MAPS*, *52*, 1722-1743. [2] Chandnani M. et al. (2019) *JGRP*, *124*, 1238-1265 [3} Chandnani M. et al. (2019) *JGRP*, *124*, 2482-2504.. [4] Robbins S. J. and Hynek B. M. (2012) *JGRP*, *117*, E05004. [5] Dickson J. L. et al. (2018) *LPSC 49*, abs. #2083. [6] Shean D. E. (2010) *GRL*, *37*, L24202. [7] Tanaka K. L. et al. (2014) *PSS*, *95*, 11–24.